Fine Structure and Physical Properties of Polyethylene Fibers in High-Speed Spinning. II. Effect of Catalyst Systems in Linear Low-Density Polyethylene

H. H. CHO,[1] K. H. KIM,[1] H. ITO,[2] T. KIKUTANI[2]

[1] Department of Textile Engineering Pusan National University, Pusan 609-735, South Korea

[2] Department of Organic and Polymeric Materials, Tokyo Institute of Technology, 2-12-1, O-okayama, Meguro-ku, Tokyo 152, Japan

Received 24 May 1999; accepted 29 October 1999

ABSTRACT: Linear low-density polyethylene (LLDPE) fibers, obtained from the melt-flow rate (g/10 min) of 45 and 50, which were polymerized by a metallocene catalyst and a Ziegler–Natta catalyst, respectively, were produced by a high-speed melt-spinning method in the range of take-up velocity from 1 to 6 km/min. The change of the fiber structure and physical properties with increasing take-up velocity was investigated through birefringence, wide-angle X-ray diffraction (WAXD), differential scanning calorimetry (DSC), a Rheovibron, and a Fafegraph-M. The birefringence increased linearly with increasing take-up velocity and that of LLDPE(45) was higher than that of LLDPE(50). With increasing take-up velocity, the crystal orientation of LLDPE transformed the *a*-axis orientation into a *c*-axis orientation. In the dynamic viscoelastic behavior of LLDPE(45) fibers with high-speed spinning, the intensity of the crystalline relaxation peak was decreased and the temperature of that was shifted lower. But that of LLDPE(50) could not be observed. The tensile strength and initial modulus were increased and the elongation was decreased with increasing take-up velocity. LLDPE(45) fibers were preferred to LLDPE(50) in mechanical properties owing to the increase of crystal and amorphous orientation factor. The change of birefringence with take-up velocity affected both the initial modulus and the tenacity uniformly. © 2000 John Wiley & Sons, Inc. J Appl Polym Sci 77: 1195–1206, 2000

Key words: LLDPE (linear low-density polyethylene); metallocene catalyst; Ziegler–Natta catalyst; high-speed melt spinning; crystal orientation; crystalline relaxation

INTRODUCTION

Polyethylene (PE) and polypropylene (PP), which are the typical of polyolefin polymers, have been little used for a general-purpose fiber except for special high-strength fibers. However, polyolefin fibers have attracted much interest since they were used for spun-bonded nonwoven fabrics. For PE, it is generally known that it is difficult to adapt it for high-speed spinning because of the rapid crystallization involved.[1]

In our recent study on high-speed spinning of HDPE among polyolefins, we accomplished high-speed spinning up to the take-up velocity of 8 km/min and the resultant fiber structure formation and physical properties were investigated. With increasing take-up velocity, the molecular orientation increased and the crystalline perfectness also increased owing to the decrease of crystalline defects in the lamella.[2]

Correspondence to: H. H. Cho.

Journal of Applied Polymer Science, Vol. 77, 1195–1206 (2000)

Generally, the linear low-density polyethylene (LLDPE) obtained from the heterogeneous Ziegler–Natta catalyst may have a linear structure including wholly short-chain branches, and, hence, the rheological properties of LLDPE are superior to those of low-density polyethylene (LDPE) obtained from the homogeneous Ziegler–Natta catalyst. Among numerous investigations, those by White and Yamane[3] and by Minoshima and White[4,5] provide extensive information about the dependence of processing behaviors on the rheological characteristics of PEs. The melt-spinning stability of PE is shown to be dependent on the molecular weight, the molecular weight distribution, and the extent of long-chain branching. Among them, the extent of long-chain branching appears to have the most significant influence on melt-spinning stability.

However, the development of the catalyst industry has brought about the appearance of the "metallocene catalyst," so-called a fourth-generation catalyst. The most important characteristics of the metallocene catalyst is that the structure and physical property of polymers obtained therefrom can be controlled by a suitable choice of the catalyst and, hence, we can design the catalyst in accordance with the final purpose. Consequently, the polymers obtained by using the metallocene catalyst are expected to have a narrower molecular weight distribution, and especially in the copolymer, the homogeneous composition can be compared to that of many other conventional catalysts. LLDPE, which is obtained from the homogeneous metallocene catalyst, compared to LLDPE from the heterogeneous Ziegler–Natta catalyst, is known to have better transparency and higher strength and a lower heat-sealing temperature. These differences in physical properties between LLDPE polymers obtained from two different catalysts are assumed to be caused by changes in the crystalline structure of the resulting polymers, namely, the LLDPE from the homogeneous metallocene catalyst is expected to have a lamella structure with a smaller thickness and more tie molecules distributed homogeneously within the fibers. Therefore, it will be possible to design a homogeneous metallocene catalyst in accordance with our purpose, because the structure and properties of LLDPE polymers thus prepared can be effectively controlled by structural changes of the catalysts used.[6–8]

In the present research, high-speed spinning has been achieved using two kinds of LLDPE polymers, LLDPE(45) from a homogeneous metallocene catalyst and LLDPE(50) from a heterogeneous Ziegler–Natta catalyst, and the fiber formation along the spinline and physical properties of as-spun fibers at various take-up speeds were investigated in comparison with each other.

EXPERIMENTAL

High-Speed Spinning

The polymers used for the high-speed spinning in the present study were LLDPE(45) and LLDPE(50) with melt-flow rates (MFR, g/min) of 45 and 50, respectively. LLDPE(45) was polymerized by a homogeneous metallocene catalyst, and LLDPE(50), by a general-purpose heterogeneous Ziegler–Natta catalyst. The LLDPE polymers were extruded from a single-hole spinneret of 0.5 mm diameter at 220°C. Mass flow rates for the two polymers were so controlled as to preserve the optimum spinning condition: for LLDPE(45), 4 g/min, and for LLDPE(50), 5 g/min. Both LLDPE(45) and LLDPE(50) were spun in the take-up speed range of 1–6 km/min. The extrusion system used was the same as that described in earlier research.[2]

Molecular Weight Distribution and Rheological Property

Average molecular weights ($\bar{M}_n$, $\bar{M}_w$) and the molecular weight distribution (MWD = $\bar{M}_w/\bar{M}_n$) of the polymer samples used were determined by using a Waters Associates GPC equipped with a high-pressure solvent delivery system (Model GPS-150C) with 1,2,4-trichlorobenzene as the eluant at 140°C. Monodisperse PS standards were used for the universal calibration. Rheological properties of as-spun fibers were measured using a Physica US 200-type rheometer according to the same procedure as in the earlier research.[2]

Fiber Structure and Physical Property

Following the same procedures as that described in the earlier research,[2] birefringence was measured by an interference microscope equipped with a polarizing filter, and mass density, by a density gradient method. Weight crystallinity (x_c)[9] was then calculated using the measured density. Equatorial X-ray diffraction profiles were obtained by a Rigaku X-ray diffractometer of D/max-III-A type with a nickel-filtered CuKα radiation source. The crystalline orientation was

Table I Characteristics of Molecular Weight and Molecular Weight Distribution for LLDPEs

Sample	$\bar{M}_n$	$\bar{M}_w$	MWD ($\bar{M}_w/\bar{M}_n$)
LLDPE(45)	25,900	67,800	2.618
LLDPE(50)	12,000	66,200	5.517

estimated by the azimuthal intensity distribution of well-resolved wide-angle X-ray reflection lines from (200) and (020) planes. Thermal analysis was performed using DSC and TMA. Stress–strain curves were obtained using a Fafegraph-M tensile machine.

RESULTS AND DISCUSSION

Molecular Weight Distribution

The number-average molecular weight, weight-average molecular weight, and molecular weight distribution of the LLDPE polymers used in this study are shown in Table I. From this table, we can see that LLDPE(45) made from a homogeneous metallocene catalyst has a higher (average) molecular weight and narrower molecular weight distribution than those of LLDPE(50) made from a heterogeneous Ziegler–Natta catalyst. This result may reflect that the activity of the metallocene catalyst is homogeneous and, hence, the length of molecular chains which have been polymerized therefrom is uniform.

Rheological Property

Changes of the complex shear viscosity with frequency for LLDPE(45) and LLDPE(50) polymers at 220°C, corresponding to the spinning temperature, are displayed in Figure 1 for comparison. Both polymers are found to exhibit the typical shear thinning phenomenon, that is, dynamic shear viscosity decreasing with increasing frequency. This is considered to arise from a disentanglement and a partial orientation of molecular chains associated with the higher frequency. The values of the dynamic shear viscosities for the two fibers are found to be nearly equal except at higher frequencies (> ca. 50 Hz), probably because they have similar MFR values. In the higher-frequency range, however, the shear viscosity of LLDPE(45) becomes larger than that of LLDPE(50), suggesting that LLDPE(45) can better

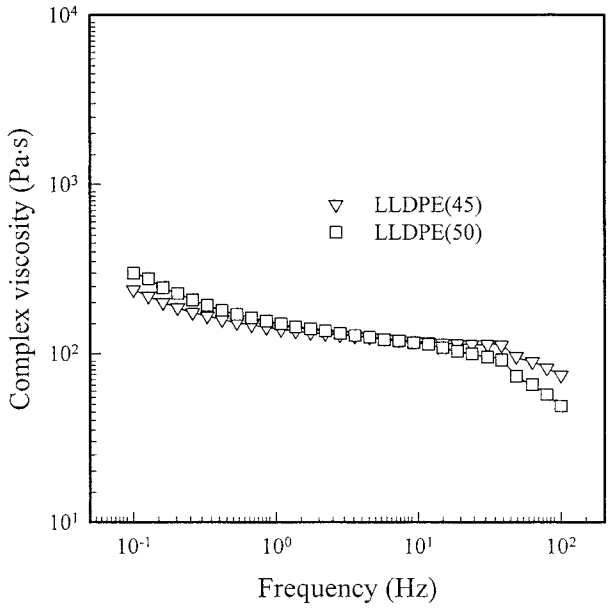

Figure 1 Complex viscosity (η^*) versus frequency for LLDPE polymers at 220°C.

stand the higher spinline tension. Figures 2 and 3 show the dependencies of the storage modulus (G') and loss modulus (G'') on the angular frequency (ω) for both LLDPE polymers at 220°C, respectively. G' and G'' are found to increase with increasing angular frequency for both cases with little difference in magnitudes. Figure 4 illus-

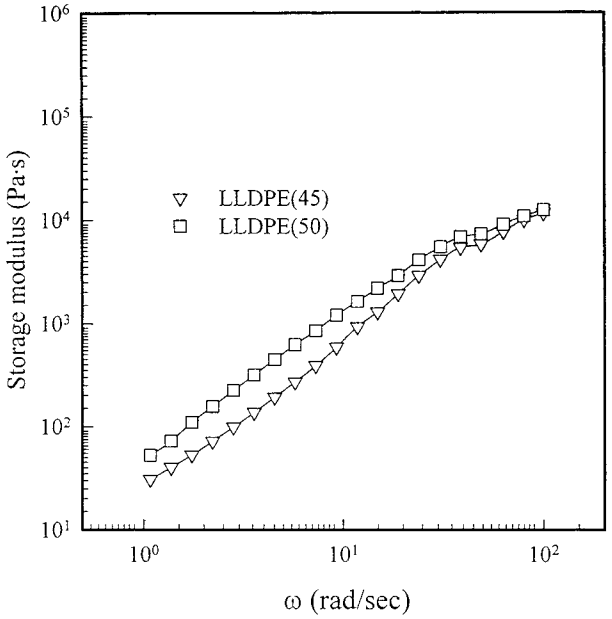

Figure 2 Storage modulus (G') versus angular frequency for LLDPE polymers at 220°C.

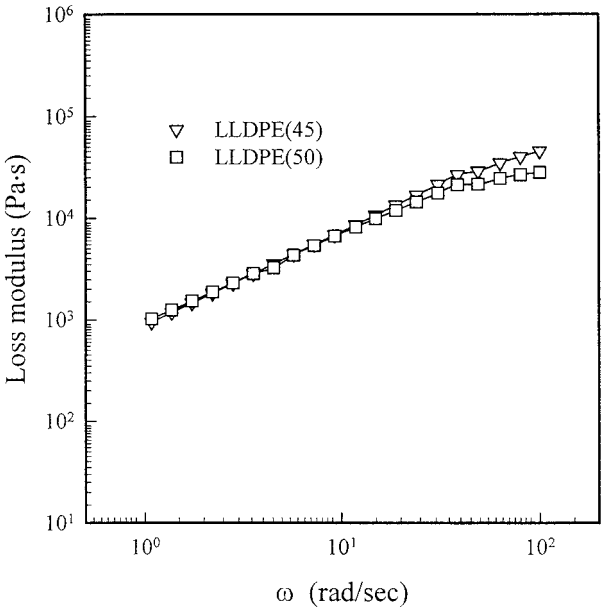

Figure 3 Loss modulus (G'') versus angular frequency for LLDPE at 220°C.

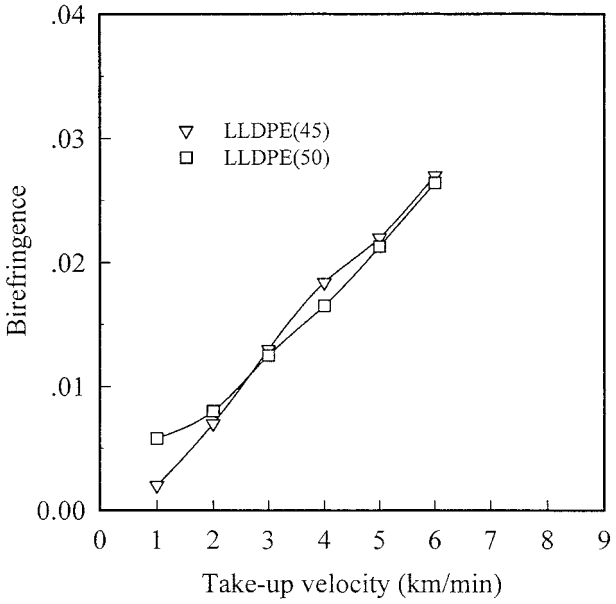

Figure 5 Relationship between birefringence and take-up velocity for LLDPE fibers.

trates the variation of tan δ with angular frequency for LLDPE(45) and LLDPE(50) polymers at 220°C, showing a similar tendency (i.e., tan δ decreasing with increasing ω) but some difference in values between the polymers over the frequency range covered.

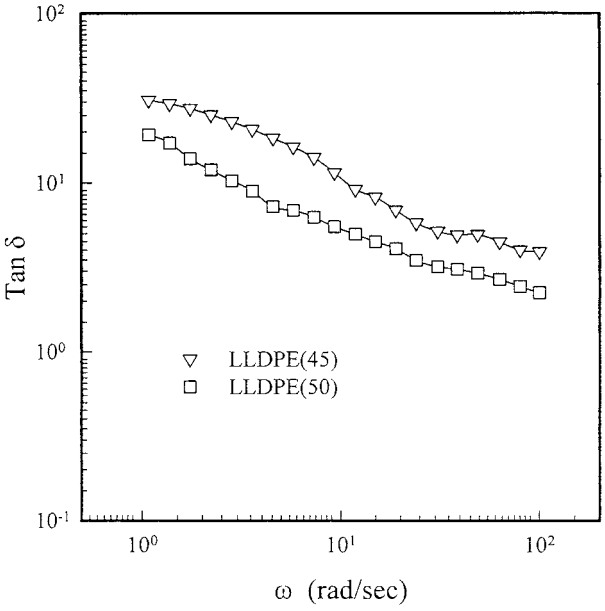

Figure 4 Tan δ versus angular frequency for LLDPE polymers at 220°C.

Molecular Orientation

Birefringence was plotted against the take-up velocity for LLDPE(45) and LLDPE(50) as-spun fibers in Figure 5. With increasing take-up velocity, the birefringences of LLDPE fibers show almost linear increases, while those of HDPE fibers showed a sigmoidal-type increase.[2] There is little difference in the values of birefringence between LLDPE(45) and LLDPE(50) fibers on the whole, but at take-up velocities above 3 km/min, the orientation of LLDPE(45) becomes better than that of LLDPE(50). It seems reasonable to speculate that the molecular orientation of LLDPE(45) gets better owing to higher molecular weight and larger extensional stress experienced in the spinline. Moreover, the enhanced molecular orientation of LLDPE(45) at higher take-up velocities would also come from the structural difference in crystalline and amorphous regions between the two fibers, that is, LLDPE(45) due to the metallocene catalyst may have lamella of smaller thickness and more tie molecules homogeneously distributed within the fibers.[6–8]

Figure 6 shows the change of density with take-up velocity. Densities of both LLDPE(45) and LLDPE(50) fibers remain nearly constant. It is expected to result from the fact that the molecular orientation by the spinline tension hardly affects changes of density because of the rapid crystallization involved as in the case of HDPE.

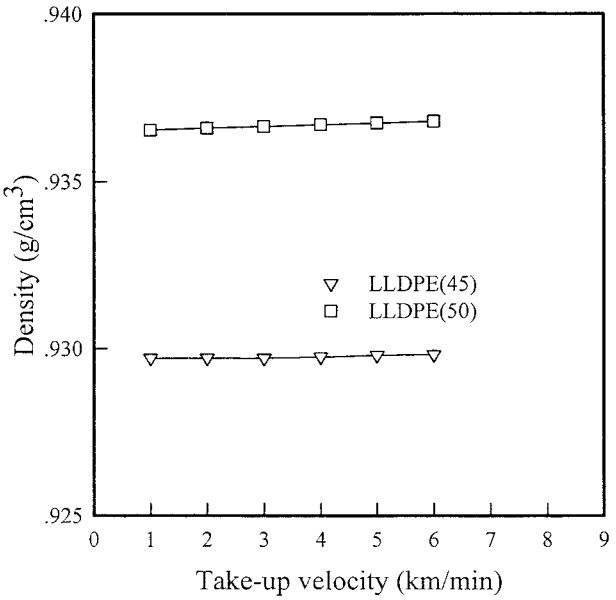

Figure 6 Relationship between (mass) density and take-up velocity for LLDPE fibers.

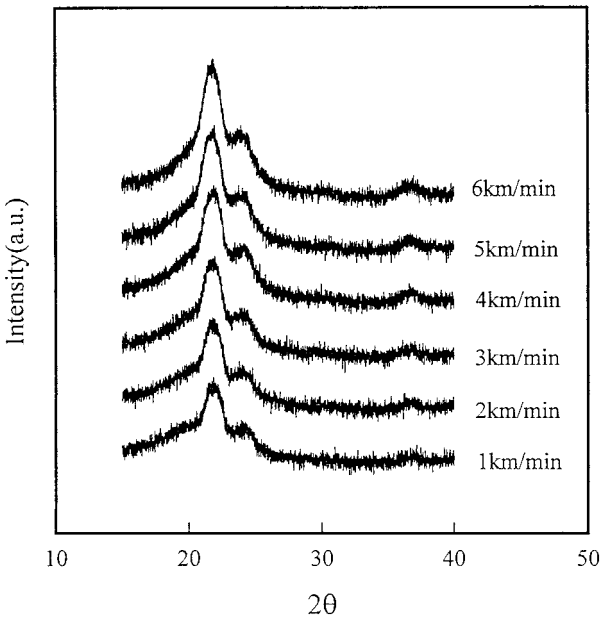

Figure 7 X-ray diffraction curves for LLDPE(45) as-spun fibers at various take-up velocities.

Figure 6 shows that the mass density of LLDPE(45) is lower than that of LLDPE(50), probably because the LLDPEs polymerized by the metallocene catalyst may possess lamella with a smaller thickness and less crystalline fraction compared to LLDPEs by the Ziegler–Natta catalyst.

Analysis of the Crystalline Structure

Figure 7 shows wide-angle X-ray diffraction of LLDPE(45) as-spun fibers from high-speed spinning. From this figure, we can observe the (100), (200), and (020) reflections at $2\theta = 21.59°$, 24.03°, and 36.30°, respectively. The profiles are the same as those of HDPE, indicating that the crystalline structure of LLDPE is similar to that of HDPE as in the result of previous research.[2] Also, the crystalline diffraction peaks are confirmed, being observed from the take-up velocity of 1 km/min. It appears that the crystalline formation at low-speed spinning is independent of an extensional stress on the spinline because of the rapid crystallization involved, like the density result in Figure 6. The diffraction peaks become sharpened with increasing take-up velocity.

Figure 8 shows wide-angle X-ray diffraction of LLDPE(50) as-spun fibers, which is similar to that of Figure 7. Presumably, this means that the ability of the crystalline formation is nearly unaffected by the type of catalyst.

Figure 9 shows changes of (weight) crystallinity with take-up velocity for the LLDPE(45) and LLDPE(50) fibers. Crystallinity remains almost unchanged independent of the take-up velocity. This may suggest that the extensional stress affects the molecular orientation up to the take-up

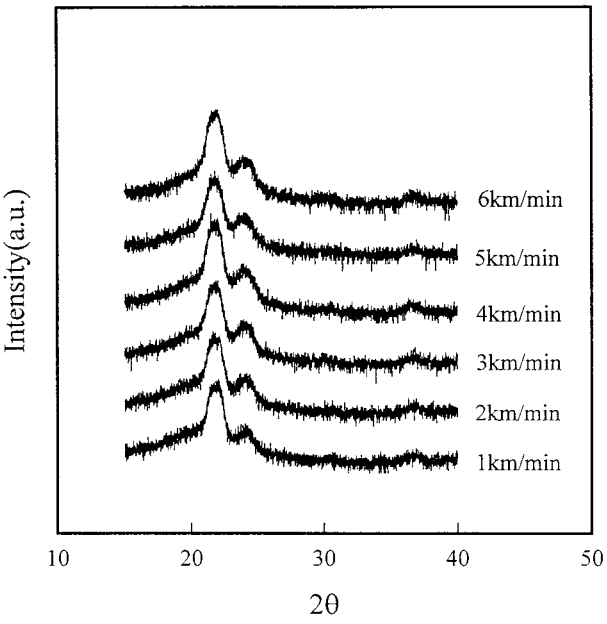

Figure 8 X-ray diffraction curves for LLDPE(50) as-spun fibers at various take-up velocities.

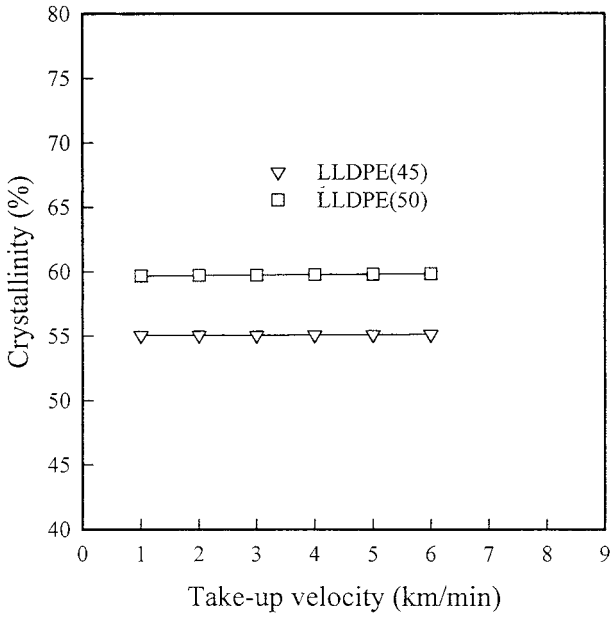

Figure 9 Relationship between (weight) crystallinity and take-up velocity for LLDPE fibers.

velocity of 6 km/min, as found in Figure 5, but affects, rarely, the crystallinity because of the rapid crystallization of the LLDPE molecules.

Figure 10 shows azimuthal diffraction curves of the (200) and (020) reflections in LLDPE(45) as-spun fibers from high-speed spinning. As judged from this figure, the (200) plane is randomly oriented up to the take-up velocity of 1 km/min and an orientation of the c-axis starts from the take-up velocity of 2 km/min, and then the orientation increases gradually with increasing take-up velocity. Figure 11 shows azimuthal scans of the (200) and (020) reflections in LLDPE(50) as-spun fibers. The crystalline orientation of LLDPE(50) is randomly oriented up to the take-up velocity of 2 km/min. The (200) plane is oriented to 15° against the fiber axis at the take-up velocity of 3 km/min, and above the take-up velocity, the plane is oriented to the c-axis, and then with increasing take-up velocity, the orientation of the c-axis gradually increases. In comparing the crystalline orientation of LLDPE(45) with that of LLDPE(50), the former is found to be better, probably owing to the larger tension experienced on the spinline. The crystalline orientation of the LLDPE(45) fiber seems to be similar to that of the HDPE(28) fiber in the results of the previous research.[2] On the whole, the orientation is believed to increase not only in the crystalline region but also in the amorphous region with increasing take-up velocity.

Figure 12 shows the changes of orientation functions f_a, f_b, and f_c with take-up velocity for the LLDPE(45) as-spun fiber. With increasing take-up velocity, f_a and f_b decrease gradually, while f_c increases. Figure 13 shows the orientation functions f_a, f_b, and f_c of the LLDPE(50) as-spun fibers as a function of take-up speed. Both f_a and f_b decrease, but f_c increases with increasing take-up velocity. Also, the f_c of LLDPE(50) is higher than that of LLDPE(45), in agreement with the results of birefringence.

Figure 14 shows the meridional X-ray diffraction profile of LLDPE(45) as-spun fibers in the scattering angle range of $2\theta = 65$–$85°$. From this figure, the (002) reflection near $2\theta = 75°$ and the (202) reflection near $2\theta = 80°$ were observed. The (202) planes are oriented to 14.7° against the fiber axis, and the leaned crystalline unit cell exists and is distributed in the range of take-up velocity of 3–5 km/min. With increasing take-up velocity, the diffraction intensity of the (002) reflection becomes larger and sharpens gradually. Figure 15 shows meridional X-ray diffraction profiles of the LLDPE(50) as-spun fibers. The intensities of

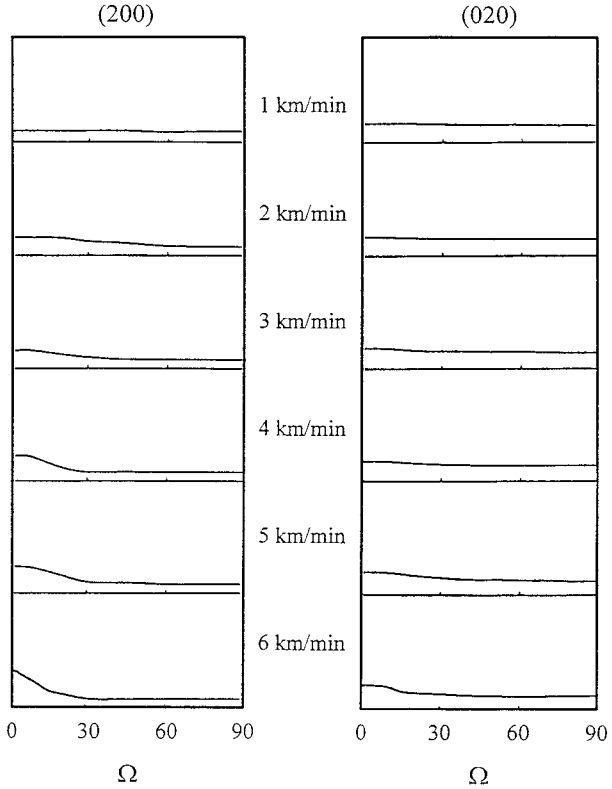

Figure 10 Variation of azimuthal profile of (200) and and (020) intensities LLDPE(45) as-spun fibers with the take-up velocity.

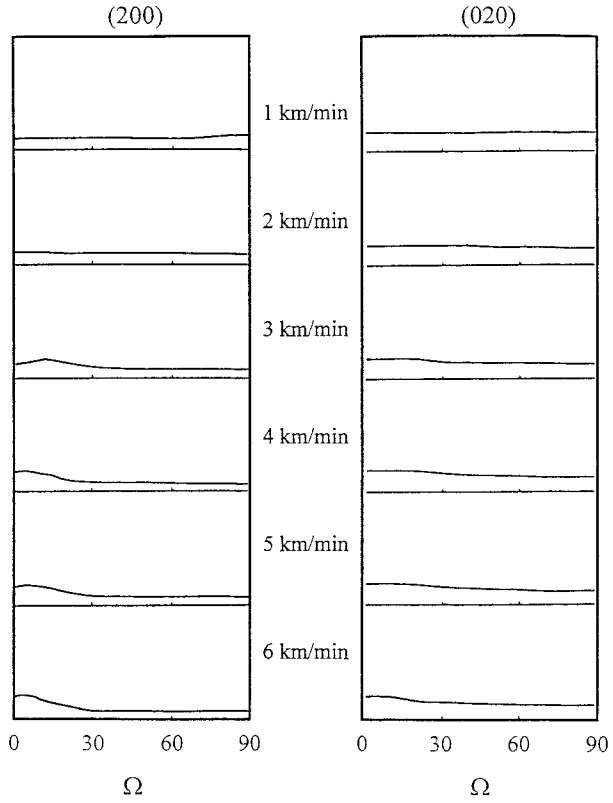

Figure 11 Variation of azimuthal profile of (200) and (020) intensities LLDPE(50) as-spun fibers with the take-up velocity.

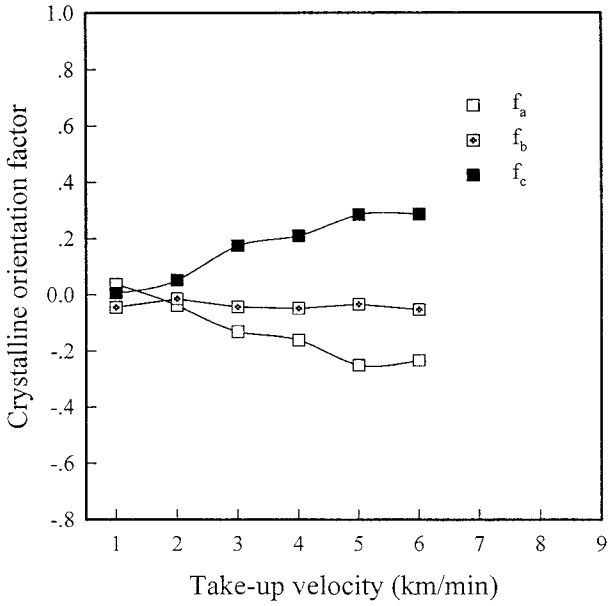

Figure 13 Crystalline orientation functions for LLDPE(50) as-spun fibers versus take-up velocity.

diffraction peaks of LLDPE(50), on the whole, turn out to be lower than those of LLDPE(45). Up to the take-up velocity of 6 km/min, the (202) reflection can be confirmed. The difference between LLDPE(45) and LLDPE(50) in the orienta-

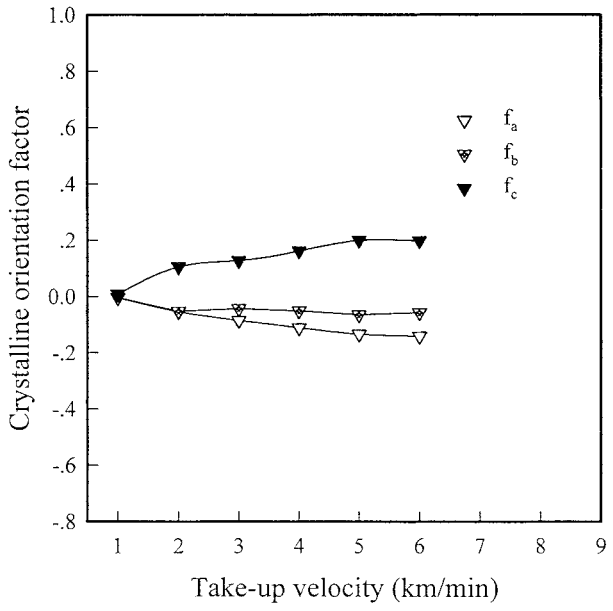

Figure 12 Crystalline orientation functions for LLDPE(45) as-spun fibers versus take-up velocity.

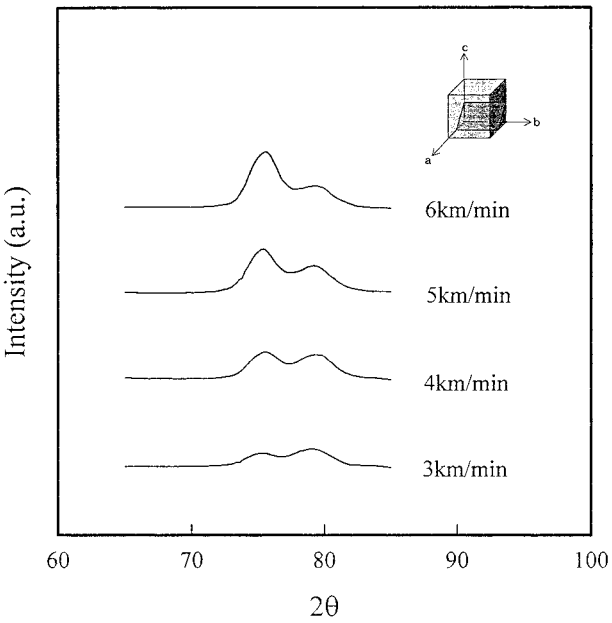

Figure 14 Dependence of wide-angle X-ray meridional scans for LLDPE(45) as-spun fibers on the take-up velocity.

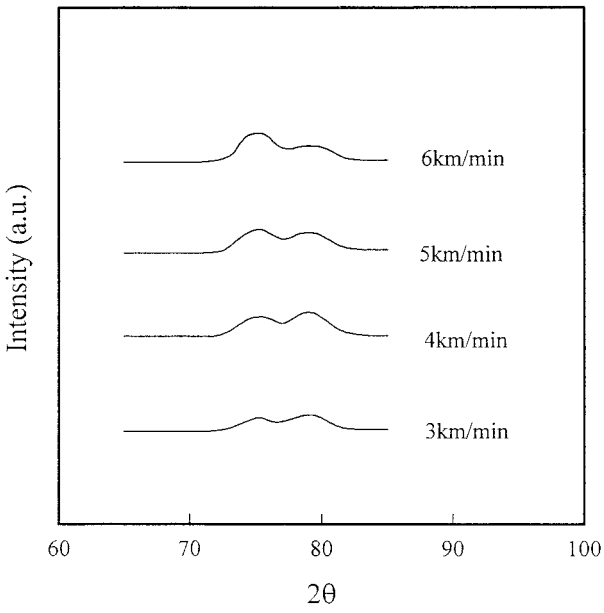

Figure 15 Dependence of wide-angle X-ray meridional scans for LLDPE(50) as-spun fibers on the take-up velocity.

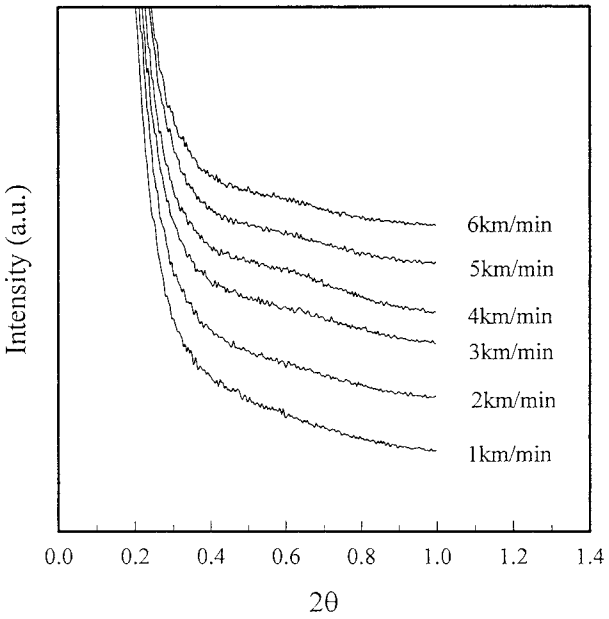

Figure 17 Change of the SAXD meridional intensity profiles of LLDPE(50) as-spun fibers with take-up velocity.

tion of crystalline unit cell may correspond to the results of density.

Figures 16 and 17 show the profiles of small-angle X-ray diffraction for LLDPE(45) and LLDPE(50) as-spun fibers, respectively, at various take-up speeds. From these figures, we cannot confirm the presence of the long periods for both fibers, suggesting that the alternative order of crystalline and amorphous regions within the fiber is random.

Figure 18 shows the amorphous orientation

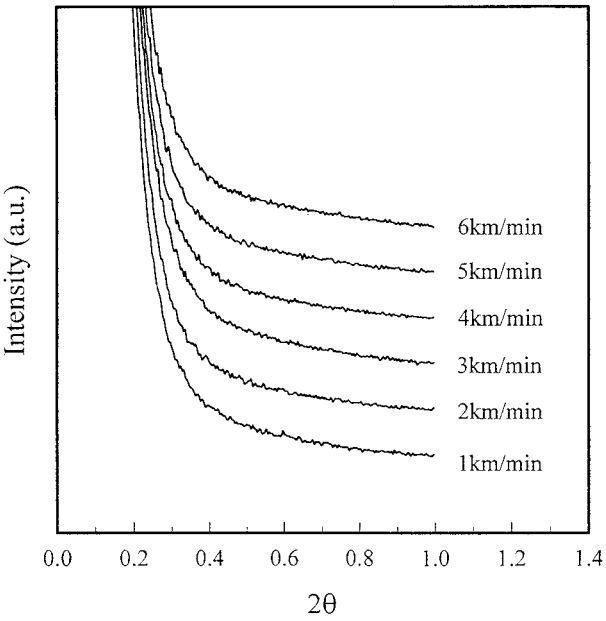

Figure 16 Change of the SAXD meridional intensity profiles of LLDPE(45) as-spun fibers with take-up velocity.

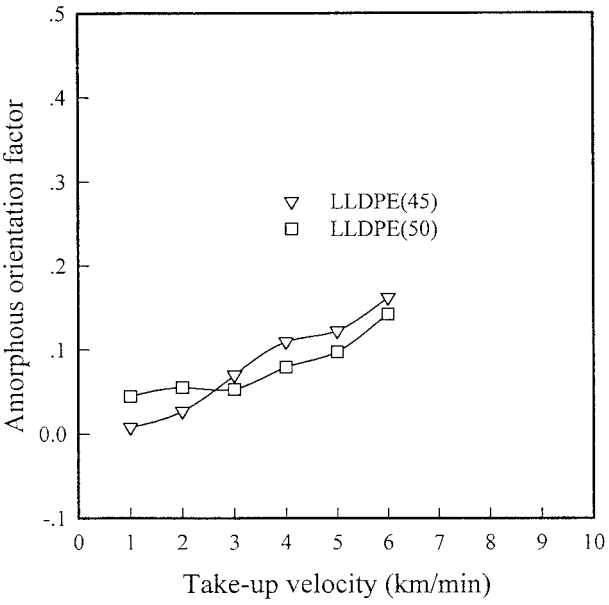

Figure 18 Relationship between amorphous orientation factor and take-up velocity for LLDPE fibers.

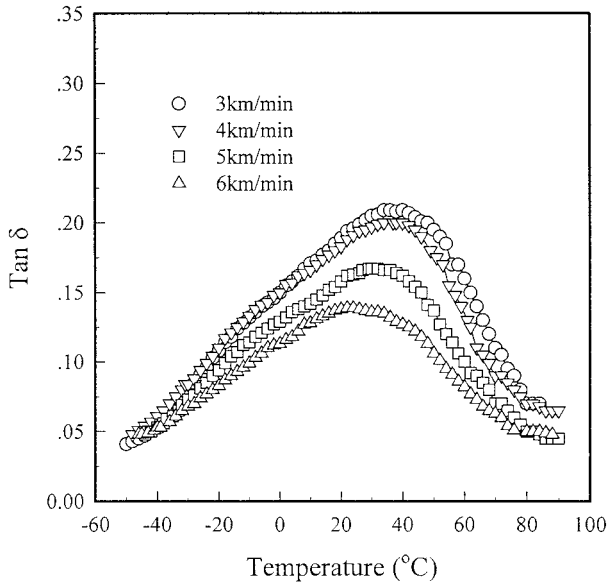

Figure 19 Effect of take-up velocity on temperature dependence of tan δ for LLDPE(45) as-spun fibers.

factor (f_a) for the LLDPE(45) and LLDPE(50) fibers as a function of take-up speed. The amorphous orientation factor was calculated by Stein's equation.[10] With increasing take-up velocity, the amorphous orientation factors of both LLDPE(45) and LLDPE(50) fibers tend to increase gradually. The amorphous orientation factor value for LLDPE(45) becomes higher than that for LLDPE(50) above the take-up velocity of 3 km/min, thereby affecting the mechanical properties of the two fibers.

Crystalline Relaxation

The crystalline relaxation behavior as expressed by the plots of tan δ versus temperature.[11–14] of the LLDPE(45) fibers spun at various take-up velocities is shown in Figure 19. The intensity of the crystalline relaxation peak decreases with increasing take-up velocity. This is considered being due to the decrease in a fraction of defects inside the crystal arising from a compactness of crystalline structure caused by increase in the take-up velocity. Generally, the crystalline relaxation peaks were observed at a little lower temperature than the melting point, but those of LLDPE(45) are observed in temperature ranges of 70–90°C lower than the melting point. From Figure 19, the crystalline relaxation peak temperature is found to shift toward the lower temperature with increasing take-up velocity, probably attributable to the fact that the structure of defects inside the crystal comes to be more disentangled and, hence, the arrangement of defects becomes easier at a higher take-up velocity. It has been confirmed that the crystalline relaxation peak of LLDPE(50) at take-up velocities of 3–6 km/min does not exist in the range of −60–110°C. The reason for this has not been discovered yet.

Thermal Property

Figures 20 and 21 show DSC thermograms of the LLDPE(45) and LLDPE(50) fibers spun at different take-up speeds, respectively. Melting temperatures of LLDPE(45) are all located near at 110°C and those of LLDPE(50) are all near 125°C at take-up speeds of 1–6 km/min. The fact that melting temperatures for both fibers are almost independent of the take-up speed may suggest that a spinline tension in high-speed spinning hardly affects the crystalline perfectness in the LLDPE fibers. The melting temperature peaks of LLDPE(45) become more sharpened and are located at temperatures lower than those of LLDPE(50), in analogy to the result of density (crystallinity). Hence, the ability of crystalline formation of the LLDPE from a metallocene catalyst needs to be studied in more detail.

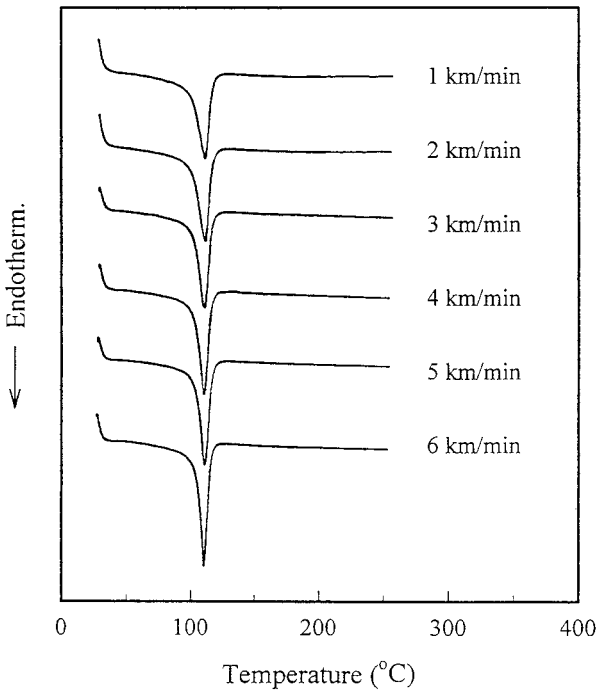

Figure 20 DSC thermograms for LLDPE(45) fibers obtained at various take-up velocities.

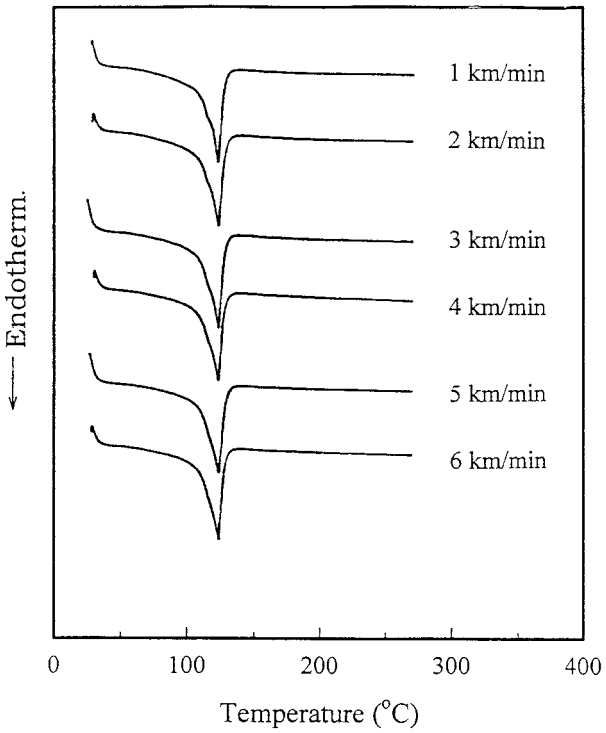

Figure 21 DSC thermograms for LLDPE(50) fibers produced at various take-up velocities.

Figures 22 and 23 show thermal shrinkages of LLDPE(45) and LLDPE(50) spun at various take-up velocities, respectively. For both LLDPE(45) and LLDPE(50) fibers, the onset points of shrinkage tend to shift to the lower with increasing take-up velocity. This means that the high-tensional amorphous chains were formed by an excess extensional stress inside fiber in high-speed spinning, and therefore, the shrinkage starts at lower temperature with increasing take-up velocity. With increasing take-up velocity, the fraction of taut-tie molecules (TTM) and the degree of shrinkage are expected to increase. Accordingly, the orientation of not only a crystalline but also an amorphous region inside the fiber will be improved as the take-up speed increases. The onset points of shrinkage for the LLDPE(45) fibers are lower than those of the LLDPE(50) fibers, reflecting that the fraction of TTM in the LLDPE(45) fiber is larger than that in LLDPE(50). Hence, it is to be expected that the fraction of TTM affects the mechanical properties of the resulting fibers.

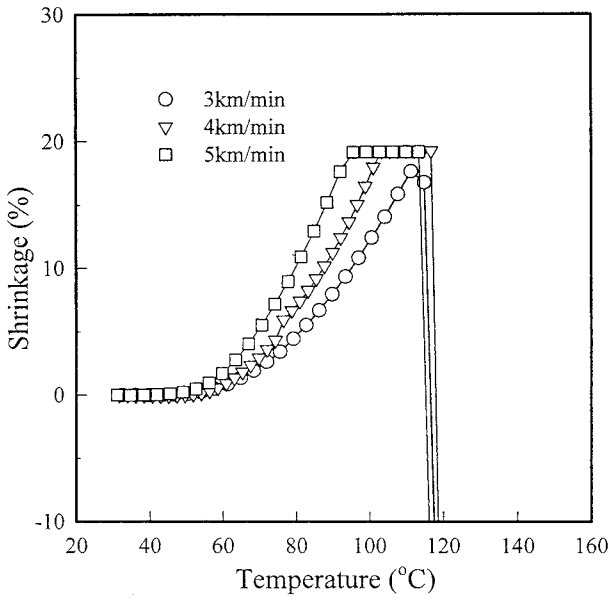

Figure 22 Shrinkage of LLDPE(45) as-spun fibers against temperature at various take-up velocities.

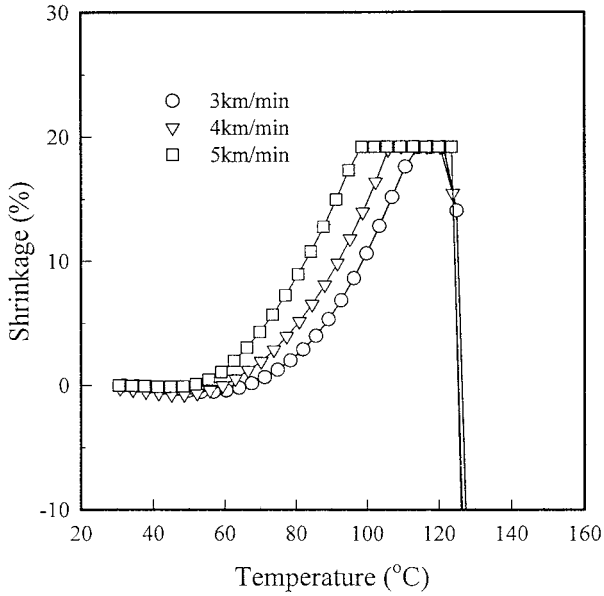

Figure 23 Shrinkage of LLDPE(50) as-spun fibers against temperature at various take-up velocities.

Tensile Property

Figures 24 and 25 show stress–strain curves of LLDPE(45) and LLDPE(50) as-spun fibers, respectively, for various take-up speeds. The data for the initial modulus, specific stress, ultimate strain, and work of rupture of the as-spun LLDPE fibers are listed in Table II. With increasing take-up velocity, the ultimate strain decreases, while both the specific stress and the initial modulus increase. This mechanical behavior may be

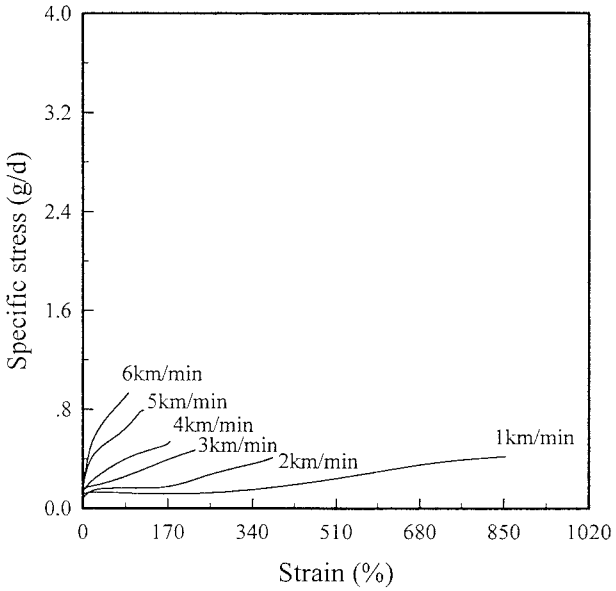

Figure 24 Stress–strain curves of LLDPE(45) as-spun fibers for various take-up speeds.

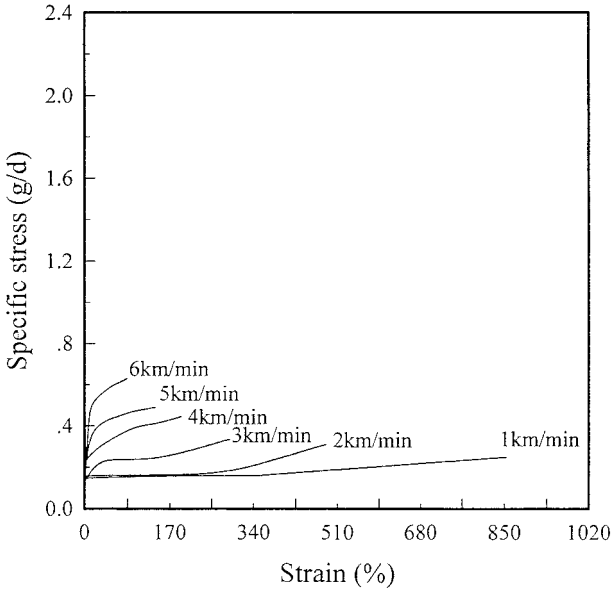

Figure 25 Stress–strain curves of LLDPE(50) as-spun fibers for various take-up speeds.

closely related to the fact that, as investigated in the other data of previous results, with increasing take-up velocity the orientation of amorphous regions in LLDPE fibers is improved and, hence, the fraction of TTM is increased. LLDPE(45), having excellent molecular orientation, is judged to have mechanical properties superior to those of LLDPE(50). There is a good correspondence between the results of birefringence and orientation. The difference in the mechanical properties between the LLDPE(45) and LLDPE(50) fibers may be associated with the difference in type of the catalyst used. In other words, the fiber-formation mechanism on the spinline will be different from each other for both cases, resulting in the difference in lamella thickness and distribution of tie molecules. Specific stress of LLDPE(45) is actually similar to that of HDPE(28) in the results of previous research.[2]

Figure 26 illustrates the relationship between birefringence and specific stress for LLDPE(45) and LLDPE(50) as-spun fibers. The specific stress of LLDPE(45) is found to be larger than that of LLDPE(50), which may be due to the increase of orientation according to orientation of amorphous chains in fibers compared to LLDPE(50).

CONCLUSIONS

High-speed spinning of LLDPE(45) and LLDPE(50) single-component fibers was carried out and the structure and physical properties of fibers spun at various take-up velocities were investi-

Table II Mechanical Properties of LLDPE Fibers in High-speed Spinning

Take-up Velocity (km/min)	Initial Modulus (g/d)		Specific Stress (g/d)		Strain (%)		Work of Rupture (g cm)	
	LLDPE(45)	LLDPE(50)	LLDPE(45)	LLDPE(50)	LLDPE(45)	LLDPE(50)	LLDPE(45)	LLDPE(50)
1	1.78	3.84	0.41	0.25	856.31	853.80	64.06	62.55
2	2.58	4.05	0.41	0.29	382.76	485.77	30.58	21.43
3	3.05	4.78	0.47	0.33	223.44	293.00	15.99	21.49
4	3.18	5.25	0.54	0.43	175.55	193.40	12.43	14.72
5	5.40	6.11	0.78	0.52	121.93	142.07	10.09	11.91
6	6.60	7.30	0.93	0.65	93.12	85.10	7.96	7.06

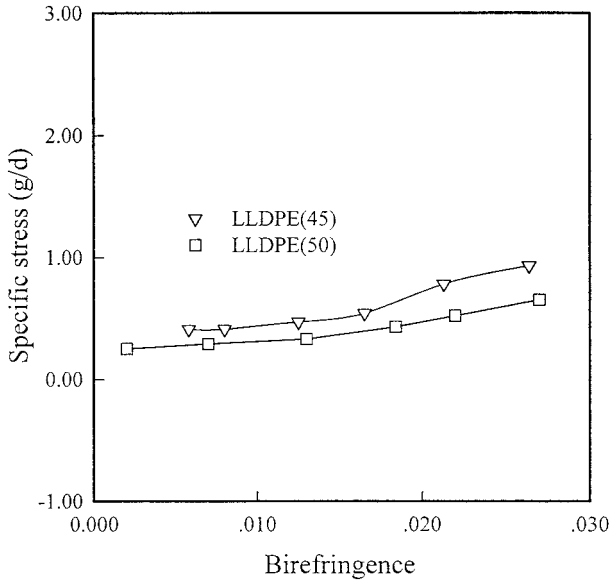

Figure 26 Relation between specific stress and birefringence for LLDPE fibers obtained from high-speed spinning.

gated through measurements of birefringence, wide-angle X-ray diffraction, DSC, dynamic viscoelasticity, tensile behavior, etc.:

1. LLDPE(45) due to the metallocene catalyst exhibited molecular orientation and physical properties superior to those of LLDPE(50) due to the heterogeneous Ziegler–Natta catalyst.
2. By an extensional stress on the spinline of high-speed spinning, the molecular orientation of as-spun LLDPE fibers increased but the crystallinity remained nearly unchanged with increasing take-up speed.
3. Despite the lower MFR of LLDPE(45), the density of LLDPE(45) was lower than that of LLDPE(50).
4. Crystalline relaxation of LLDPE(45) was observed in temperature range of 70–90°C lower than the melting point.

REFERENCES

1. Ziabicki, A.; Kawai, H. High-Speed Fiber Spinning; Wiley: New York, 1985; Chapter 15.
2. Cho, H. H.; Kim, K. H.; Ito, H.; Kikutani, T. J Appl Polym Sci, in press.
3. White, J. L.; Yamane, H. J Appl Chem 1987, 59, 193.
4. Minoshima, W.; White, J. L. J Non-Newton Fluid Mech 1986, 19, 251.
5. Minoshima, W.; White, J. L. J Non-Newton Fluid Mech 1986, 19, 275.
6. Sasaki, T.; Johoji, H. Kobunsi 1993, 42, 907.
7. Kashiwa, N. In Metallocenes as Promising Catalysts for New Generation of Polyolefins; Soga, K., Ed.; CMC, Tokyo, 1993; p 25.
8. Kashiwa, N. In International Symposium on Catalyst Design for Tailor-Made Polyolefins, JAIST, March, 1994.
9. Beret, S.; Prausnitz, J. M. Macromolecules 1975, 8, 536.
10. Stein, R. S. J Polym Sci 1959, 34, 709.
11. Iwayanagi, S.; Miura, I. Jpn J Appl Phys 1965, 4, 94.
12. Sinnott, K. M. J Appl Phys 1966, 37, 3385.
13. Takayanagi, M.; Matsuo, T. J Macromol Sci-Phys B 1967, 1, 407.
14. Sinnott, K. M. J Polym Sci C 1966, 14, 141.